**Distribution Agreement**

In presenting this thesis as a partial fulfillment of the requirements for a degree from Emory University, I hereby grant to Emory University and its agents the non-exclusive license to archive, make accessible, and display my thesis in whole or in part in all forms of media, now or hereafter now, including display on the World Wide Web. I understand that I may select some access restrictions as part of the online submission of this thesis. I retain all ownership rights to the copyright of the thesis. I also retain the right to use in future works (such as articles or books) all or part of this thesis.

Washington Huang Apr. 10, 2024

**Multi-unit Analysis of Homeostatic Plasticity Impairments and FXS Within Mouse Somatosensory Barrels and Septa**

by

Washington Huang

Peter Wenner, PhD.
Adviser

Neuroscience and Behavioral Biology

Peter Wenner, PhD.
Adviser

Chris Rodger, PhD.
Committee Member

Megan Massa, PhD.
Committee Member

2024

**Multi-unit Analysis of Homeostatic Plasticity Impairments and FXS Within Mouse Somatosensory Barrels and Septa**

by

Washington Huang

Peter Wenner, PhD.
Adviser

An abstract of
a thesis submitted to the Faculty of Emory College of Arts and Sciences
of Emory University in partial fulfillment
of the requirements of the degree of
Bachelor of Sciences with Honors

Neuroscience and Behavioral Biology

2024

# Multi-unit Analysis of Homeostatic Plasticity Impairments and FXS Within Mouse Somatosensory Barrels and Septa

By Washington Huang

***Importance:*** Autism Spectrum Disorder (ASD) is a prevalent neurodevelopmental condition with no known cure, affecting 1 in 100 individuals worldwide. Fragile X Syndrome (FXS), a common inherited neurodevelopmental disorder, is often co-diagnosed with ASD and is characterized by cognitive, motor, and neural plasticity impairments. This research focuses on understanding the impacts of FXS on neural networks and homeostatic plasticity within the barrels and septa of the mouse somatosensory cortex, areas crucial for processing whisker sensory stimuli and eliciting whisker motor movements.

***Objective:*** This study aims to elucidate the role and functionality of homeostatic plasticity in the septal regions compared to the well-studied barrel regions of the somatosensory cortex in FXS models. Specifically, it investigates the effects of FXS on baseline neural activity and responses following whisker deprivation.

***Methods:*** Multi-unit recording data from extracellular neural recording probes placed in the barrel cortex of wild-type and *Fmr1* Knockout (KO) mice were collected under both whisker-deprived and non-deprived conditions at two time points (Postnatal age P16 and P21). Whiskers were stimulated at six different velocities. Histology was performed to determine probe placement in the barrel cortex. Data was analyzed by creating velocity response curves (VRCs) for each condition.

***Main hypothesis:*** Multi-unit activity within the barrels and septa will have similar homeostatic plasticity responses following whisker deprivation in wild-type subjects, while *Fmr1* KO would lead to a larger neural activity decrease in the septa when compared to barrels.

***Results:*** The investigation into homeostatic plasticity within the barrel and septa in FXS models faced significant challenges due to insufficient sample sizes across multiple experimental conditions, preventing statistical significance. Consequently, this limitation hindered the ability to support or reject the main hypothesis.

***Conclusion:*** This study underscores the inherent complexities and limitations of employing multi-unit analysis to explore intricate neurological phenomena such as homeostatic plasticity in the context of FXS. This research journey highlighted the crucial need for larger sample sizes and more refined methodologies when studying homeostatic plasticity and FXS within the somatosensory cortex. Nonetheless, the study represents a novel examination of the septa and paves the way for future studies to unravel the complexity of homeostatic plasticity and FXS.

# Multi-unit Analysis of Homeostatic Plasticity Impairments and FXS Within Mouse Somatosensory Barrels and Septa

by

Washington Huang

Peter Wenner, PhD.
Adviser

A thesis submitted to the Faculty of Emory College of Arts and Sciences
of Emory University in partial fulfillment
of the requirements of the degree of
Bachelor of Sciences with Honors

Neuroscience and Behavioral Biology

2024

Acknowledgements

I want to thank Dr. Peter Wenner and Alishah Lakhani for providing me with this invaluable opportunity to pursue my research interests and conduct research in the Wenner lab. Furthermore, I sincerely appreciate all the motivation, care, expertise, time, and knowledge that have been dedicated to me to ensure my personal and academic growth along with my project completion.

I want to thank Dr. Megan Massa for supporting and providing me with the skills and knowledge to critically analyze, compose, and confidently present my research project.

I want to thank Dr. Chris Rodgers, Dr. Carlos Gonzalez-Islas, and Dr. Dobromila Pekala for all the invaluable insights and suggestions provided throughout my research project.

## Table of Contents

## Introduction

### Fragile X Syndrome

According to a Centers for Disease Control and Prevention surveillance summary published in 2023, around 1 in every 36 children within the United States has been diagnosed with autism spectrum disorder (ASD) (Maenner et al., 2023). Worldwide, the number is estimated to be 1 in every 100, where males diagnosed with ASD outnumber females 4 to 1. ASD is a developmental condition associated with various social, behavioral, and neurological processing/ integrating conditions that vary along a spectrum. Due to these conditions, individuals with ASD are often faced with a variety of impacting societal stigmas, ranging from ignorance to prejudice to discrimination (Turnock et al., 2022). ASD is often identified early in development, at around 18-24 months of age. Early diagnosis distinguishes ASD symptoms from other types of potential neurodevelopmental delays or conditions (Zeidan et al., 2022; Amaral, 2017). While ASD is prevalent in our society, unfortunately, there are currently no known treatments for autism due to its complex pathological nature.

Fragile X Syndrome (FXS), the most common form of inherited neurodevelopmental disorder, is often associated with cognitive and language problems and is frequently co-diagnosed with ASD (Rogers et al., 2001). In males, there is around a 50% co-diagnosis rate; in females, the percentage drops to around 20%. FXS is caused by a CGG repeat sequence found on the 5' untranslated region of the *Fmr1* gene on the X chromosome, leading to the inactivation of this gene and an absence of the Fragile X Messenger Ribonucleoprotein 1 (FMRP) (Kaufmann et al., 2017; Deosthale et al., 2023). FMRP is an RNA-binding protein that plays an essential role in neural plasticity and architecture. As a gene expression regulator, FMRP is involved in the proliferation and specification of neurons, axonal targeting, dendritic protein synthesis regulation, and white matter development. In addition, the absence of FMRP has also been

associated with hyperexcitability in the neural circuit. Since FMRP is crucial in maintaining synaptic plasticity, patients diagnosed with FXS often have malfunctioning neuronal circuits in signal reception, processing, and integration (Richter et al., 2021).

Plasticity

In the nervous system, two primary forms of plasticity exist. Correlation-based Hebbian plasticity is widely known as the mechanism through which new information can be processed and retained (Fox et al., 2017). The mechanism behind the famous phrase "Cells that fire together, wire together," stated by Hebb, is that simultaneous presynaptic and postsynaptic activity strengthens synapses (Lisman, 2017). Through this coincidental activity, learning and reinforcement could occur. On the other hand, homeostatic plasticity is also crucial to ensuring neuronal homeostasis, the tendency of neurons to maintain a target level of electrical activity. Using intrinsic and synaptic modulations to adjust excitatory and inhibitory responses, homeostatic plasticity can compensate for sudden neuronal perturbations and maintain a set threshold. These two plasticity mechanisms allow the nervous system to adapt to new inputs while maintaining optimal function (Fox et al., 2017). However, both Hebbian and homeostatic plasticity are prone to failure in FXS cortical cultures (Martin et al., 2012; Bülow et al., 2019).

In terms of Hebbian plasticity, FXS's adverse impacts have been shown primarily on the synaptic side, where FMRP is responsible for the regulation of metabotropic glutamate receptor (mGluR) protein synthesis. As such, according to the mGluR theory of FXS, when there is an absence of FMRP, a negative regulator of protein synthesis, it leads to an exaggeration of long-term depression (LTD) in the hippocampus. This leads to epilepsy, developmental delay, and cognitive impairment, which are key features of FXS (Bear et al., 2004).

Homeostatic plasticity is also impaired in FXS due to both post-natal developmental disruptions of brain circuits and FMRP losses that elicit molecular and synaptic dysregulation. Because a variety of the genes that encode homeostatic plasticity molecules are targets of FMRP, the loss imbalances network activity and alters synaptic/intrinsic plasticity (Liu et al., 2022; Niere et al., 2012). When looking at homeostatic plasticity, homeostatic synaptic plasticity and homeostatic intrinsic plasticity both work together to ensure neural homeostasis. Whereas homeostatic synaptic plasticity focuses on the modulation of synaptic strength to maintain a set state (Turrigiano, 2011), homeostatic intrinsic plasticity pertains to the neuron's ability to adjust membrane excitability to achieve a similar goal (Bülow et al., 2019; Desai, 2003). Past studies have shown that FXS is disruptive in both synaptic and intrinsic plasticity, together leading to overall homeostatic malfunctions (Soden et al., 2010; Bülow et al., 2019).

In homeostatic synaptic plasticity, a decrease in synaptic activity leads to a subsequent increase in AMPAR production (Soden et al., 2010). Termed synaptic scaling (Turrigiano et al., 1998), this mechanism allows neurons to detect changes in activity and consequently adjust receptor trafficking on the postsynaptic side (Soden et al., 2010; Liu et al., 2022). The FMRP KO model, with an absence of FMRP, demonstrates impaired homeostatic synaptic plasticity to adequately compensate for neural perturbations. This finding was further corroborated in a later study on human neurons, where FMRP KO led to impaired synaptic plasticity that was subsequently repaired through *Fmr1* gene repair (Soden et al., 2010; Zhang et al., 2018).

In homeostatic intrinsic plasticity, ion channels in the membrane are adjusted in response to changes in activity levels to moderate membrane excitability. Through this alteration, neuron features such as firing rate and patterns can be maintained in stable conditions (Desai et al., 1999). Aside from modulating AMPA receptors, FMRP can also adjust sodium and potassium ion

channels (Contractor et al., 2015). Whereas in normal circumstances, a decrease in sensory input converts single spiking neurons into multi-spiking neurons through ion channel modulation, this conversion is absent in *Fmr1* KO cortical cultures. However, while multi-spiking neurons also increase their spiking rate, *Fmr1* KO exaggerates this transition process (Bülow et al., 2019). These two opposing results again highlight HIP's impairments in FXS and the complexities behind such impairments.

Barrel/ Septa Research

Previous research into homeostatic plasticity has primarily utilized the mouse model due to its ease of manipulation, genomic understanding, and fast reproduction cycles. Mice have a barrel cortex, which is the whisker-responsive area of the somatosensory cortex. As mice primarily depend on their whiskers to "see the world," perturbations to the whiskers are an area of focus for homeostatic plasticity somatosensory studies. Acting as a cortical representation of the whiskers located on the mouse's contralateral snout, the barrel field consists of a grid of barrels (high concentration of neurons) divided by the septa (low concentration of neurons). Somatotopically organized into rows and columns, each individual barrel is thought to show a preference for a specific whisker known as the columnar whisker (CW) (Rice et al., 1977; Bureau et al., 2008). Research into the barrel field has illustrated that the barrels primarily encode spatiotemporal information received through CW interactions with external stimuli (Alloway, 2007).

While the somatosensory cortex is organized into six specific layers, each having specific input-output connections and varying roles, layer 4 is where the barrel field is located. Due to the higher density of neurons found in individual barrels, when compared to the surrounding septa, it

appears darker under microscopy and can be visually identified (Petersen, 2007). Layer 4 acts as the first level of processing for sensory signals. Furthermore, neurons within layer 4 are mainly localized to the barrel they are located in, without significant cross-barrel axonal bridges (Petersen et al., 2000). Driven by the activity of layer 4, layer 2/3 of the barrel cortex is responsible for integrating sensory information from varying barrels and whiskers, as the neurons found in layer 2/3 are interconnected, with dendritic connections to adjacent barrel areas (Kim et al., 2016; Varani et al., 2021). Layer 5 cells are identified as the barrel cortex's main output layer, where the neurons send signals to other cortical and subcortical brain regions. Furthermore, layer 5 neurons are known to be the only neurons with dendrites crossing into all six layers of the cortex, receiving inputs from all layers (Shai et al., 2015; Moberg et al., 2022).

Whisker deprivation has been widely used as a method of sensory deprivation to study neuronal plasticity. As neurons undergo changes, homeostatic plasticity should maintain a firing rate. Thus, sensory deprivation through whisker trimming would lead to increased neuronal sensitivity and homeostatic plasticity will facilitate the excitation. In a study looking at layer 2/3 and layer 5 of the barrel cortex, whisker deprivation induced homeostatic plasticity in the form of synaptic scaling (Glazewski et al., 2017). This synaptic adjustment, however, is impaired in FXS models (Soden et al., 2010). Furthermore, it is shown that for 2-week-old *Fmr1* KO subjects, the ascending neural projections connecting layer 4 to layer 2/3 were malfunctioning in regard to strength and connection probability. However, by week 3, this projection is similar to wild-type mice, indicating *Fmr1*'s role in shaping sensory circuits during a critical period where neural processing development is especially dependent on experience or environmental factors (Bureau et al., 2008).

Currently, most FXS and ASD research in the somatosensory cortex has been focused on the barrel due to its clear sensory input and established research literature. However, the septa are underemphasized despite having a crucial role in sensory processing. In a prominent 2021 review on the barrel field and its neuronal circuits, the authors mentioned that septal region connections are still "enigmatic" (Staiger et al., 2021). Past research suggests that the primary role of septa is the integrating and processing of signals across multiple barrels and encoding the kinematics of whisker movements, such as frequency and velocity. While it may seem similar to that of layer 2/3 of the barrel, as septal cells possess dendrites and axons that span across multiple barrel borders, it has been found that distinct circuitries exist for the barrel and septal columns. Whereas inter-barrel projections originating from barrels are short-ranged, mainly reaching only the surrounding barrels, septal column projections extend 2-3 barrel distances along the row of whisker representation (Alloway, 2007).

Furthermore, while layer 4 barrels are mainly excluded from inter-barrel connections, the septa act as the connectors of inter-barrel projection from neighboring barrels and septa (Brecht et al., 2002; Kim et al., 1999). Expanding on this dual circuit concept, the septal circuit is also responsible for processing and delivering barrel cortex information to varying motor brain regions to regulate mouse whisking behaviors (Alloway, 2007). Although the barrel and septa circuits are two different processing streams, they work together to discriminate objects by both passive and active whisker movements, with a cooperative mechanism that is yet to be elucidated (Alloway, 2007). Considering that ASD and FXS patients have also been shown to have difficulty when integrating perceptive motion signals and demonstrate impaired movement, alluding to impaired signal integration and output, an investigation of the septa's role and

FMRP's influences could shed new light on the pathology and behavioral conditions associated with both FXS and ASD.

Research Direction

In light of the sparse research that has been conducted on the septa, for my research, I am primarily interested in the neural circuitry and functioning of the septa. In particular, I am interested in examining whether homeostatic plasticity in the septa is similar to that of the barrel and how FXS impacts baseline neural activity and activity following whisker deprivation. Utilizing the multi-unit data from a probe placed into the barrel field, I am able to extract neuronal activity in response to varying levels of sensory stimulation in two genotypes (wildtype and *Fmr1* KO) and whisker manipulation conditions (non-whisker-deprived and whisker-deprived). As my research project is similar to my lab's ongoing research analyzing single-unit data into homeostatic plasticity and FXS in the barrel column, I will be taking advantage of the septa data previously deemed unusable.

For my research project, the main hypothesis is as follows: Multi-unit activity within the barrels and septa will have similar homeostatic plasticity responses following whisker deprivation in wild-type subjects, while *Fmr1* KO would lead to a larger neural activity decrease in the septa when compared to barrels. I have three predictions that aim to test my main hypothesis. The first prediction is that neurons in the barrel and septa will demonstrate an increase in neural activity in whisker-deprived WT subjects compared to non-whisker-deprived WT subjects. This prediction is based on the idea that homeostatic plasticity functions similarly in both the barrel and the septa in WT. The second prediction is that at baseline, without any whisker deprivation, barrel activity will decrease in FXS subjects compared to WT subjects, and

that septa activity will show a stronger decrease in activity in FXS subjects. This second prediction is primarily concerned with FXS's impairing role in the neural network integrity of both barrel and septa, with the septa experiencing a larger effect. Lastly, the third prediction is that for whisker deprivation, barrel activity will decrease in FXS whisker-deprived subjects compared to WT whisker-deprived subjects, and that septa activity will show a stronger decrease in FXS subjects. This final prediction looks at homeostatic plasticity's sensitivity to FXS impairments for both the barrel and septa, with the septa having a larger impact due to its sensory integration role. Through these three predictions, I will be able to identify and compare both the role of homeostatic plasticity and FXS found within the septa to that of the barrel.

## Methods

### Subjects

Male wild-type (WT) and *Fmr1* knockout (KO) mice were bred, kept, and tracked at a designated facility on campus. Mice were genotyped at P14 to determine if they were WT or KO. For each of these groups, there will be *Fmr1* KO subjects that are both whisker-deprived and non-whisker-deprived, along with their WT counterparts. Once again, the experimental condition of the mice is unknown until genotyping, which ensures experimental blinding. Whisker deprivation is performed on the right side of the mice belonging to the whisker-deprived groups. To ensure deprivation throughout the lifespan, the whisker length is kept around 2mm with trimmings that occur every other day under light isoflurane anesthesia starting on P14. Prior to *in vivo* recordings on either P16 or P21 through random assignment, whiskers are allowed to grow for 2-3 days to facilitate the following stimulation and recording procedure.

Extracellular Recording

In preparation for *in vivo* neuronal recordings, the mouse is first placed in an isoflurane chamber, where it is anesthetized. Chlorprothixene sedative is administered during this step as well. After ensuring the effectiveness of anesthesia through a pinch test, the subject is transported to a heating pad where optimal body temperature is kept. The head is subsequently fixed onto an apparatus that ensures both stability and a constant flow of isoflurane to maintain anesthesia. A craniotomy is then performed over the barrel cortex (3mm lateral, 1.5mm caudal from bregma) on the left hemisphere to gain access to the brain. A 64-channel Cambridge Neurotech probe stained with fluorescent DiI (1mg in 1mL of ethanol) is then inserted blindly at a 60-degree angle (to the horizon) to record the activity of L2/3, L4, and L5/6 neurons of the barrel cortex.

Before initiating the electrophysiological recording, the best whisker (BW) of the day is initially estimated by manually stimulating whiskers and identifying which whisker elicits the strongest response. Although the columnar whisker (CW) is the whisker that is somatotopically associated with the barrel that the probe is in, the CW is not always the same as the BW. FXS models have suggested a decreased likelihood of instances where the CW is the BW (24% compared to 53% in WT) (Antoine et al., 2019). Thus, we chose to examine the responsiveness of the BW of the day responses instead of the CW. Upon estimating the BW, our lab-made 3x3 piezoelectric stimulator array is attached to 9 whiskers, with the BW ideally located at the center. The contraption mentioned above was made in reference to the design highlighted by Jacob et al., 2010. The BW of the day (whisker that elicits the strongest response across all probe channels) is then verified through piezo and subsequently stimulated 50 times each at six different velocities (up to 800 degrees per second), along with no stimulation (0 degrees).

Histology

Once extracellular recordings have been completed, the mouse is euthanized through decapitation. In order to preserve barrel cortex integrity, the following steps must be completed in a timely manner, utilizing ice for low temperatures whenever possible. Once decapitated, the head is dropped into a 1x PBS solution surrounded by ice to chill while the base layer of an agar cube container can be prepared and allowed to solidify. While solidifying, the mouse brain is extracted. The brain is then oriented and placed on top of the agar, followed by the addition of more agar to fully submerge the brain. Upon solidification, the brain is first placed onto the sagittal plane, where an anterior agar cut tangent to the barrel field location is made. The brain is then placed on a protractor on its coronal plane, with the anterior of the brain going into the protractor. A 30-degree cut is made into the right hemisphere using a protractor, aligning the top of the barrel field directly upwards. The orienting cut method was inspired by Agmon et al.'s 1991 paper, which developed this method to prepare mouse somatosensory forebrain slices.

The agar-enclosed brain is then placed on an ice-cooled vibratome, and 4-5 225um slices are extracted while submerged in a 1x PBS environment. The slices are subsequently mounted and imaged on a Keyence fluorescence microscope, where the DiI stain location can be identified along with the barrel cortex. Figures 1a and 1b represent images taken from the fluorescence microscope, with Figure 1a depicting a barrel probe location and Figure 1b depicting a septa probe location. Utilizing the histology result, I can categorize the subject into either barrel or septa groups. Developed during my time at Wenner lab, this represents a novel histology and imaging method that allowed me to identify the barrel field without any form of staining or fixing. Through keeping the histology on ice for the entire procedure, the barrels were

preserved for nearly an hour on microscope slides prior to fading. While identifying the probe still required fluorescence, the histology method cut down on both time and devoted resources.

Data Analysis

To analyze the raw data collected with TDT (Tucker-Davis Technologies) systems, the tdt library is utilized to convert binary data into Python structures, which is the environment utilized extensively throughout the project. Velocity response curves (VRC) are then calculated for the BW of the day data. The 50 ms after the velocity-specific stimulation was averaged for each subject, and baseline activity (the average spiking in the 50 ms period before the stimulation) was subtracted from this average. The error bars represent the standard error of the mean (SEM) across subjects for each experimental condition. An average VRC was created for all experimental groups to demonstrate the amount of spiking from 0 to 800 degrees/sec. For each individual velocity, considering non-parametric data and small sample sizes, a Mann-Whitney U Test is subsequently utilized to identify potential significance with a 95% confidence ($p<0.05$).

**Results**

Velocity response curve (VRC) data from both P16 (Figures 2-6) and P21 (Figures 7-11) were statistically compared with genotype (WT and KO) and whisker manipulation (WD for whisker-deprived and nWD for non-whisker-deprived) conditions to identify trends and patterns. Given that developmental time plays a crucial role in homeostatic plasticity development and the ability of neural circuits to adapt and adjust to sensory perturbations properly, I will discuss the VRC data of P16 and P21 separately.

P16 VRC Results

An organized distribution of P16 subjects in all combinations of genotype and whisker deprivation conditions can be found in Table 1. Since probe insertion into the barrel cortex is performed blindly, I was unable to obtain any KO WD subjects whose probe landed in the septa at P16. Due to this limitation, a statistical comparison could not be made utilizing that experimental group.

Overall, when analyzing the P16 multi-unit VRC data, most experimental group comparisons did not demonstrate any significant deviations of average spike counts at any of the velocities ranging from 0 to 797 deg/sec. In addressing my first prediction, looking at whisker manipulation for WT subjects in both the barrel and septa, it can be shown that for the barrel comparison, no large activity difference is noted despite being well-powered with relatively high sample sizes (Figure 2). This observation was also noted for the septal comparison - while the WD condition trends higher, the overlapping SEM error bars prevent a different conclusion from being drawn (Figure 3).

For my second prediction, which compares genotypes for nWD groups, a well-powered trend variation can be observed in the barrel. For the barrel VRC comparison between WT and KO of nWD, an overall decrease in neural activity is depicted for the KO group compared to the WT (Figure 4). Furthermore, a statistically significant difference was also identified at 65 degrees/ second, where the WT group's response was stronger than the KO group. This result, however, is not displayed in the septa. For the septa's comparison, besides displaying no variability in trend for WT and KO, only one sample was collected for the KO nWD experimental condition (Figure 5).

Lastly, in addressing my third prediction on homeostatic plasticity FXS impairments, I compared genotypes for WD groups. When looking at the barrel VRC comparison between WT and KO for WD, it can be shown that there is no observable activity difference across all velocities despite the KO condition depicting a slightly lower activity level (Figure 6). When looking at the septa VRC comparison, I was unable to see a trend comparison as I did not receive any subjects that fell under the category of KO WD during my data collection. As such, a septa comparison was not possible.

P21 VRC Results

An organized table for the P21 subjects with all genotypes and whisker deprivation conditions can be found in Table 2. Similar to P16 data, due to the blind insertion of the recording probe and the smaller size of the septa compared to barrels, data collection from septa is rarer. In addition, as with the P16 data, a small and uneven number of subjects for all genotypes and whisker manipulation conditions makes deriving statistical significance difficult. While a few relatively well-powered comparisons can be identified in P16 (sample size greater than 3 for both comparison groups), this was not seen in the data collected for P21. Nonetheless, preliminary trends and guiding analyses can still be made.

In addressing my first prediction utilizing P21 VRC data, an interesting trend was identified for the barrel comparison. For this comparison, which looked at the influence of whisker manipulation on WT neural activity levels, the data displayed an overall lower activity level for the WD condition when compared to the nWD (Figure 7). This trend, however, is not seen in the same comparison made within the septa. For the septa VRC comparison, WD

displayed a higher neural activity level than nWD (Figure 8). It must be noted that for nWD, only one set of subject data was collected.

For the second prediction that compares genotype variations of VRC trend for nWD, a difference can be identified for the barrels. The collected data shows that for barrel comparison, the KO group has a noticeably lower activity level when compared to the WT (Figure 9). However, when utilizing this finding to compare to that of the septa data, the limited sample size prevented any result insights to be drawn. For the septa comparison, only one sample was collected for KO and WT each, making noteworthy trend discrimination difficult.

Finally, utilizing the P21 VRC to answer my third prediction, which will be looking at the difference between genotypes for WD, a trend difference can be noted between the barrel and the septa. In the barrel, it is observed that at all velocities, the activity levels or responsiveness was no different between the WD KO and WT as the error bars were overlapping (Figure 10). This was not the case when looking at the same septa comparison. In the septa, it is found that for all velocities, the KO group displayed a lower evoked neural response than the WT (Figure 11). This was the closest we could come to showing a difference between the septa and barrel responses.

Overall Results

Consolidating the results for P16 and P21, two overall trend differences can be observed in the response strength following whisker stimulation. First, when comparing septal to barrel data, a difference in activity level can be seen for the barrel and septa at the two time points of P16 and P21. Whereas for P16, septal activity levels were overall, on average, lower than the barrel, this trend is absent at P21, as both barrel and septal levels were similar. Furthermore,

when comparing P16 to P21's barrel activity levels, P21's activity strength, in general, seemed lower than that of P16.

In conclusion, although the number of experimental subjects available represented a significant restriction on statistical significance, we were still able to test some of my predictions at the developmental age of P16 and P21. In addressing prediction 1, while no deviation is identified for whisker manipulation in both the barrel and septa for P16 WT subjects, the same trend is depicted for both barrel and septa, with the barrel comparison being well-powered. P21's lone subject for WT nWD in septa did not allow a conclusion to be drawn. For prediction 2, while both P16 and P21's barrel comparison of genotype for nWD yielded the same trend of KO mice demonstrating lower activity levels, along with P16's data achieving statistical significance, there is an overall lack of comparable septa data due to sample size. Lastly, for prediction 3, P21's VRC identified a trend variation of KO activity decrease in the septa comparison of genotype difference for WD that is not seen within the barrel. Once again, this comparison could not be made in P16 as there was a complete lack of KO WD subjects for the septa.

**Discussion**

While the mouse's somatosensory barrel cortex has been a significant target of homeostatic plasticity and FXS research, researchers have been primarily focused on the barrel columns, with little attention being given to the septa due to the barrel's clear sensory output, ease of access, and established data/ research methods (Staiger er al., 2021). In light of this, by utilizing velocity response curves, this research project represents a novel dive into the septa's neural functioning and how homeostatic plasticity and FXS play a role at two important developmental periods of P16 and P21. Whereas P16 represents the maturation of layer 4 in the

barrel cortex, P21 provides a more complete maturation of the entire barrel cortex (Erzurumlu et al., 2013; Jamann et al., 2021).

Although for both P16 and P21, varying comparisons between and within barrel/septa VRC results could not be made due to the lack of experimental condition data, both expected and unexpected trends were observed for the possible comparisons. For example, in both P16 and P21's barrel data that compare WT and KO for nWD (Figures 4 and 9), with P16's data being well-powered, the decrease in neural activity of the KO compared to WT is reflective of the absence of FMRP in single unit data and previous works (Richter et al., 2021; Antoine et al., 2019). This alignment can further be seen in P21's septa data comparing genotype for WD subjects, with the KO exhibiting lower neural activity reflecting barrel studies that demonstrate impairment influences that FXS has on homeostatic plasticity (Figure 11) (Liu et al., 2022). However, in P16 data, despite our lab's single unit recording and past literature (Fox et al., 2017) highlighting that WD is associated with increased excitability in WT conditions, the well-powered multiunit data collected for P16 barrel (Figure 2) says otherwise. This thus introduces the questioning of both the sample size, particularly that of the septa, and the utilization of multiunit recordings for homeostatic plasticity and FXS measurements. Nonetheless, this uncertainty of statistical significance prevents me from providing neither solid support nor rejection of the main research hypothesis utilizing P16 or P21 VRC data.

Previous research into homeostatic plasticity has emphasized that upon sensory deprivation, a perturbation would increase the signal strength due to excitatory compensations that have developed (Fox et al., 2017). While this may be the case, the multiunit VRC data I collected from P21 showed a drastically opposite trend. In the P21 barrel VRC graphs comparing whisker manipulation for WT subjects (Figure 7), it was found that nWD individuals had, on

average, a higher signal strength than the WD individuals. While this multi-unit result contradicts past single-cell analyses and established literature, it is possible that the multi-unit analysis was able to depict a decrease in overall stimulus-driven activity. This has been seen in Sieben et al.'s 2015 paper on rat tactile input restriction's impact toward somatosensory processing, where prenatal trimming followed by neuronal recording at P19-22 depicted decreased overall sensory-evoked responses in the supragranular layers (layers 1-3) of S1 (Sieben et al., 2015). However, the lack of statistical significance and utilization of multiunit analysis still play the main culprit in this observation and thus will be further discussed in the limitations.

Limitations

As mentioned, the number of experimental subjects and recording method were two of the biggest limitations that affected my research project. Throughout my research, sample collection proved to be a challenge as for each mouse subject, the genotype and recording position were not known until after the experiment. While genotype uncertainty prevents data analysis bias, probe position uncertainty is mainly due to the barrel field, visibly observed in layer IV of the somatosensory cortex, being hidden until post-mortem histology. Furthermore, with time constraints and uncontrollable events such as mice rubbing off their whiskers, abnormal electrophysiological noise, and varying sensitivity to isoflurane, the ideal number of subjects for each varying experimental condition was not adequately met. As such, despite trying to control for individual variability with the subtraction of baseline neural activity, when experimental groups were statistically compared, the lack of subjects for varying experimental groups made statistical significance difficult.

The other limitation that significantly impacted the clarity of the data I collected was the utilization of multiunit analysis compared to single-unit recordings. Originally, when devising the experimental setup, the decision to utilize multiunit analysis was primarily due to the limited time and resources that I had. As my project was concurrent with my mentor's current research into single-unit recordings of the mouse somatosensory barrel, we decided that since investigating the septa is still a novel endeavor, a broad-picture multiunit analysis might be adequate. Furthermore, utilizing multiunit data analysis presents a convenient yet valuable approach that takes advantage of experimental data deemed unusable by my mentor's research paradigm and attempts to identify whether septa data reflects homeostatic plasticity and FXS similarly to that of the barrel. However, through utilizing multiunit data, where any spiking activity past the threshold is measured and recorded, a lot of in-depth neuronal-specific analysis and layer-specific activity is lost.

In previous single-cell recording experiments pertaining to homeostatic plasticity, it has been noted that synaptic excitatory/ inhibitory ratio (E/I ratio) balance plays a crucial role in maintaining optimal firing rates. For *Fmr1* KO subjects, an observed increase in E/I ratio was attributed to the hyperexcitability found in experiments. Furthermore, Antoine et al., 2019 pointed to the decrease of feedforward inhibitory firing as a culprit for the E/I ratio increase (Antoine et al., 2019). While this is a crucial step in better elucidating the underlying cause of impaired homeostatic plasticity and potentially that of autism patients, this differentiation is unable to be seen in multiunit recordings. As in the case of multiunit recordings, the inability to differentiate between excitatory and inhibitory signals may lead to blurred data interpretation. For example, an increase in inhibitory firing will be identified as an increase of neuronal firing in

general through multiunit recording, leading to an overall increase in VRC, which may be interpreted oppositely to that of single-unit analysis.

Another limitation of utilizing multiunit data comes from being unable to differentiate between the best whisker of the day and the best whisker of the unit. Considering that the best whisker of the day compiles neural activity across all channels and identifies the whisker that elicits the strongest response overall, the strongest responding whisker may simply be caused by it having the greatest number of associated neurons surrounding the probe. As such, utilizing multiunit recordings introduces the possibility that the selected best whisker of the day is not the best whisker of the unit, which is the actual neural representation that responds the strongest to the stimulated whisker. The only way to truly identify the type and property of the most responsive neuron, the neuron most sensitive to said whisker stimulation, is to look at the unit level.

In addition, while histology enables me to discern between barrel and septa experiment groups for test subjects, histology also plays a critical role in my mentor's single-unit analysis. In a barrel experiment, a distinction can be made between the best whisker of the day and that of the columnar whisker (CW), which is the whisker-corresponding barrel in which the probe is physically located. While the CW was previously believed to be the same as the BW, research has shown that the CW is not always the BW, as neurons within a barrel can respond to whiskers other than the CW. In addition, FXS models have suggested a decreased likelihood of instances in which the CW is the BW (24% for KO compared to 53% in WT) (Antoine et al., 2019). This significant neurophysiological change associated with FXS models also cannot be discerned by multiunit recordings, further limiting the multiunit method's scope.

Lastly, utilizing multiunit recordings prevents layer-specific differentiation, which plays a significant role in analyzing homeostatic plasticity and FXS's influence on signal input/output and integration. The barrel cortex is divided into six different layers, each having a specific role and function when integrating stimuli information received from the whiskers. For instance, in barrel layers 2/3, the neurons are primarily responsible for integrating signals from surrounding barrels, with axons and dendrites that cross into adjacent barrel areas (Kim et al., 2016). Layers 4/5, on the other hand, particularly layer 4, house the neurons that span across the barrel column and are responsible for the initial cortical processing of sensory signals (Scala et al., 2019). When looking at septal space, on the other hand, layer 4 is primarily responsible for multi-whisker sensory information input through the paralemniscal pathway, highlighting a potentially varying circuit to that of the lemniscal pathway found in barrels (Alloway, 2007). Utilizing this information, it can be shown that layer-specific functions are significantly varied with different properties and actions in both the barrel and the septa, with the barrel's lemniscal pathway invigorating layer 3 to layer 6 and the septa's paralemniscal pathway invigorating layers 1 to layer 5 (Alloway, 2007). Thus, summating all the layers together through multiunit data analysis may not be the most accurate interpretation of homeostatic plasticity functioning and FXS impacts.

**Future Direction & Conclusion**

Throughout this research project, aside from attempting to provide a preliminary analysis into the role of homeostatic plasticity and the influences of FXS found within the cortex septa, it also provided a methodological analysis on the importance of single unit recordings when it comes to the highly complex and dynamic role that defines homeostatic plasticity. Taking into

consideration the results and limitations, while multicell recordings can provide general indicators of neural functioning, a large enough sample size is needed to dissuade experimental variability and statistical insignificance. Furthermore, the multiunit results must be approached with a grain of salt and verified with more specific single-unit recordings. Although the results found in this research project could not support or reject my hypotheses, the septa still deserve the attention of future experimental endeavors as they play a crucial role in multi-sensory integration and motor coordination and output. Considering that ASD patients are often found with difficulty in integrating multiple sensory inputs caused by neural deficits, along with difficulty in motor control, septa research could potentially shed light on the underlying neural causes and bring us a step closer to identifying and treating ASD.

Moving forward, future studies should utilize single-unit recordings to further target and identify cell-specific synaptic and intrinsic mechanisms that are at play in septal areas. In addition, when addressing the difficulty of localizing the much harder-to-reach septal space, previous research has utilized intrinsic signal optical imaging (Antoine et al., 2019). While this method was not utilized in our lab, localization plays a much more significant role when attempting to record from septa. Through this endeavor, and along with the constant advancement of homeostatic plasticity/ FXS research and new technological methods, the "enigmatic" world of the barrel septa could become fruitful in contributing to cracking the code of ASD.

## Figures and Graphs

| P16 Subjects | Wildtype | | Fmr 1 KO | |
|---|---|---|---|---|
| **Non-Whisker-Deprived** | Barrel: 4 | Septa: 3 | Barrel: 4 | Septa: 1 |
| **Whisker-Deprived** | Barrel: 7 | Septa: 2 | Barrel: 2 | Septa: 0 |

*Table 1:* Subject distribution chart showing the number of P16 subjects pertaining to each experimental group, separated by barrel and septa.

| P21 Subjects | Wildtype | | Fmr 1 KO | |
|---|---|---|---|---|
| **Non-Whisker-Deprived** | Barrel: 5 | Septa: 1 | Barrel: 2 | Septa: 1 |
| **Whisker-Deprived** | Barrel: 2 | Septa: 4 | Barrel: 5 | Septa: 2 |

*Table 2:* Subject distribution chart showing the number of P21 subjects pertaining to each experimental group, separated by barrel and septa.

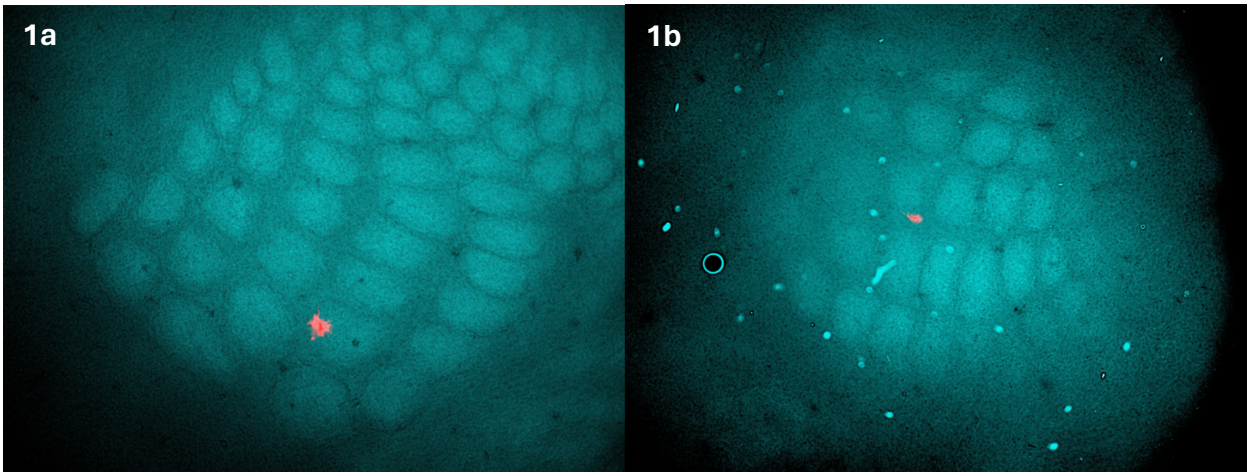


*Figure 1:* Fluorescence images of barrel cortex and probe (marked by DiI) landing in a barrel (left, 1a) and septa (right, 1b). Both images were taken under a Keyence fluorescence microscope. The DiI marker is identified utilizing a Cy3 filter cube.

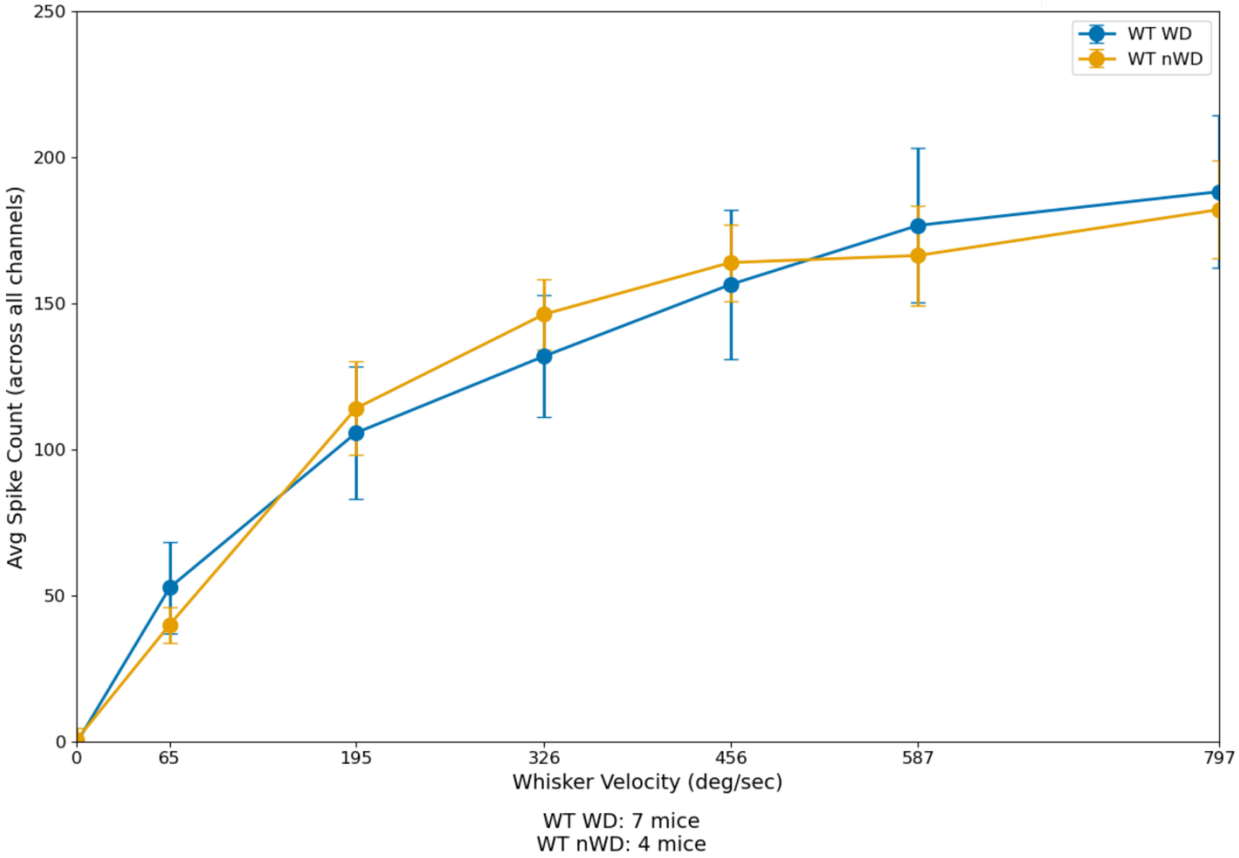


*Figure 2:* Velocity response curve (VRC) for **P16 wildtype subject barrels** comparing whisker deprivation and non-whisker deprivation. The y-axis represents the average spike counts across all channels for all files at each velocity pertaining to a specific experimental group, and the x-axis represents the varying stimuli velocities utilized from 0 to 800 degrees per section. The error bars shown for each point represent the standard error of the mean (SEM). * Indicates a Mann-Whitney U test significance of $p<0.05$.

.

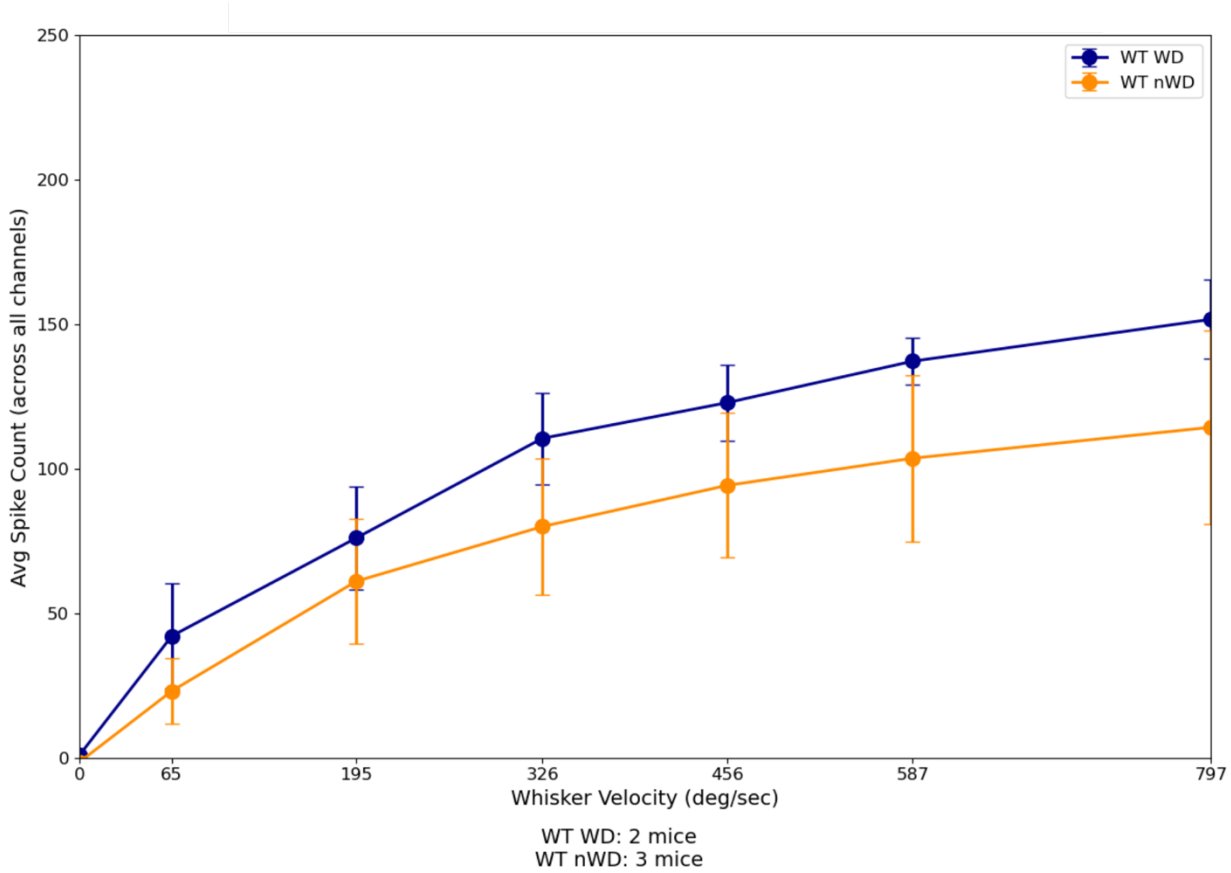


*Figure 3:* Velocity response curve (VRC) for **P16 wildtype subject septa** comparing whisker deprivation and non-whisker deprivation. The y-axis represents the average spike counts across all channels for all files at each velocity pertaining to a specific experimental group, and the x-axis represents the varying stimuli velocities utilized from 0 to 800 degrees per section. The error bars shown for each point represent the standard error of the mean (SEM). * Indicates a Mann-Whitney U test significance of $p<0.05$.

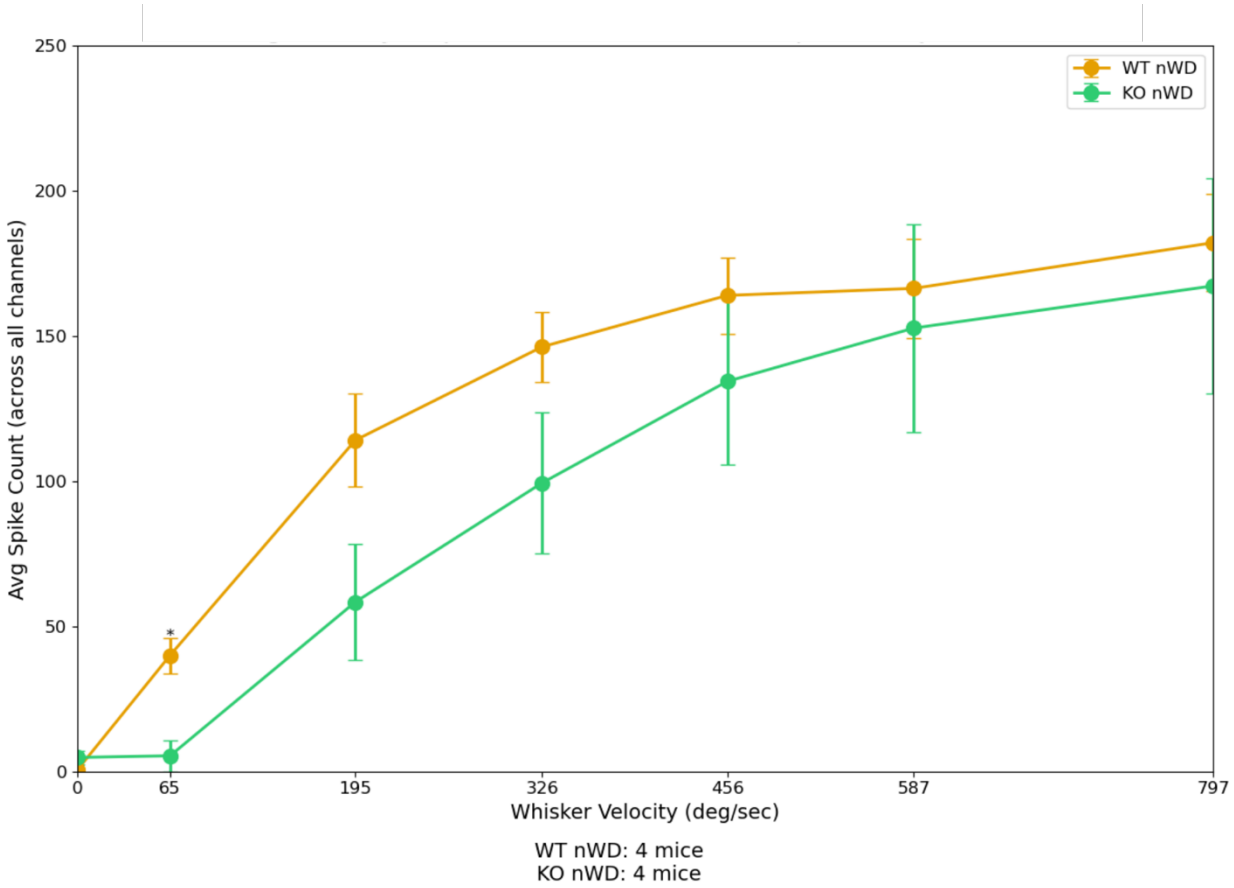


*Figure 4:* Velocity response curve (VRC) for **P16 non-whisker-deprived subject barrels** comparing wildtype and knockout genotypes. The y-axis represents the average spike counts across all channels for all files at each velocity pertaining to a specific experimental group, and the x-axis represents the varying stimuli velocities utilized from 0 to 800 degrees per section. The error bars shown for each point represent the standard error of the mean (SEM). * Indicates a Mann-Whitney U test significance of $p<0.05$

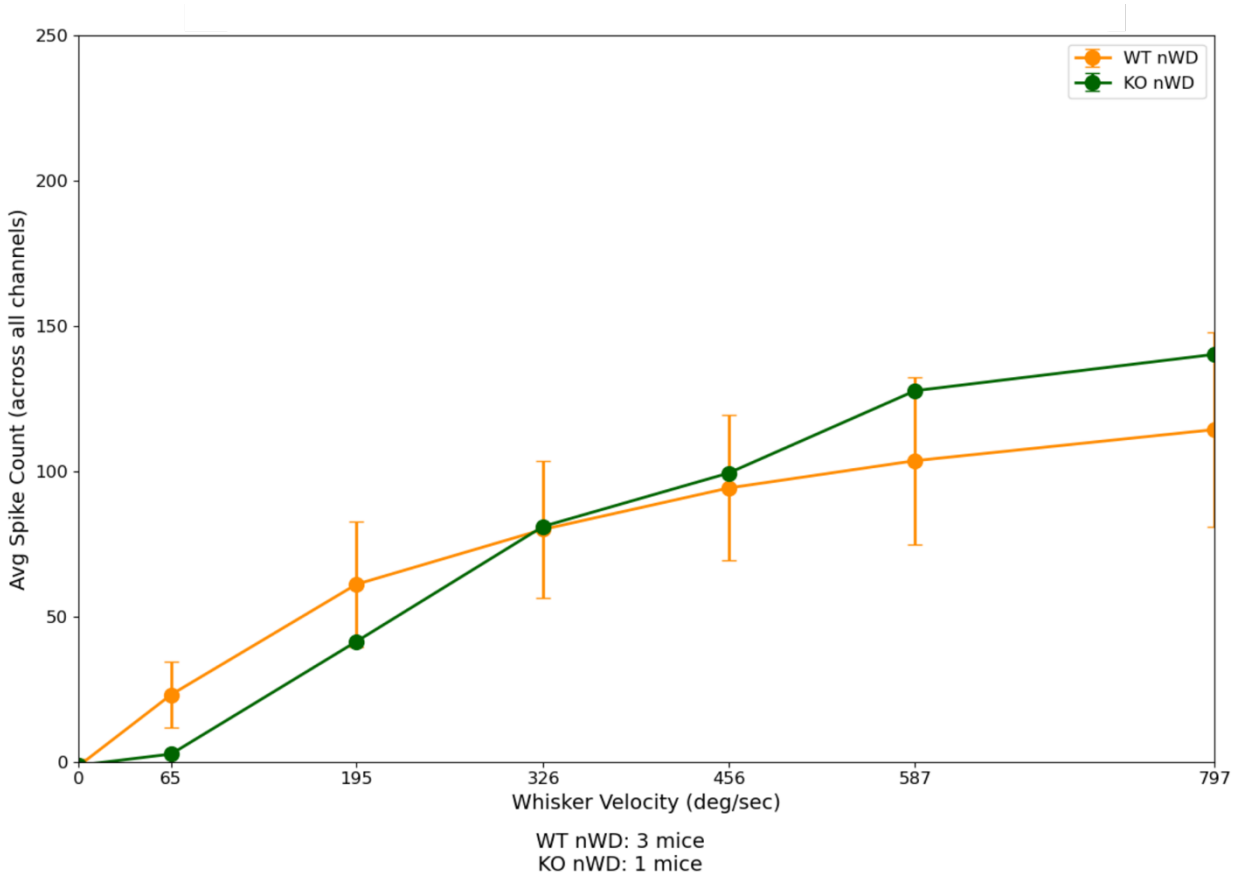


*Figure 5:* Velocity response curve (VRC) for **P16 non-whisker-deprived subject septa** comparing wildtype and knockout genotypes. The y-axis represents the average spike counts across all channels for all files at each velocity pertaining to a specific experimental group, and the x-axis represents the varying stimuli velocities utilized from 0 to 800 degrees per section. The error bars shown for each point represent the standard error of the mean (SEM). * Indicates a Mann-Whitney U test significance of $p<0.05$.

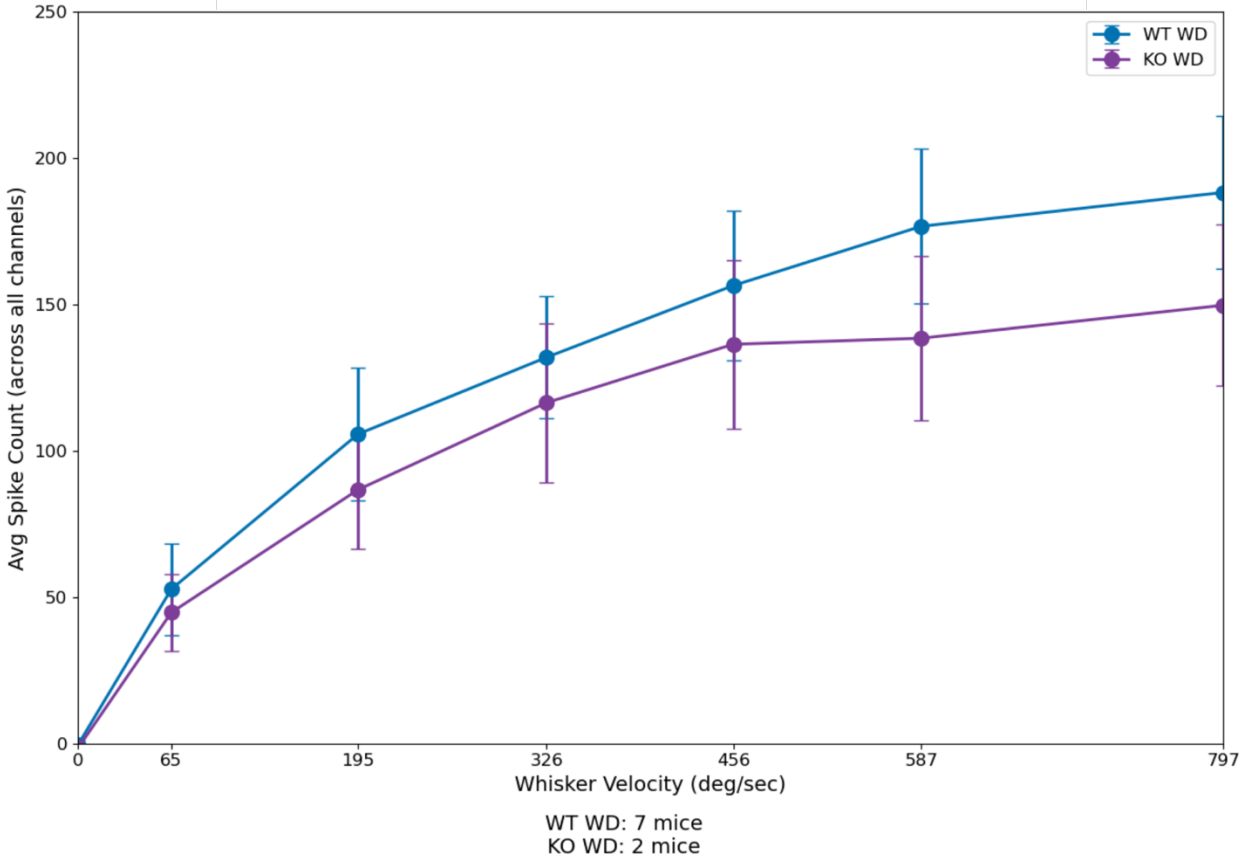


*Figure 6:* Velocity response curve (VRC) for **P16 whisker-deprived subject barrels** comparing wildtype and knockout genotypes. The y-axis represents the average spike counts across all channels for all files at each velocity pertaining to a specific experimental group, and the x-axis represents the varying stimuli velocities utilized from 0 to 800 degrees per section. The error bars shown for each point represent the standard error of the mean (SEM). * Indicates a Mann-Whitney U test significance of $p<0.05$.

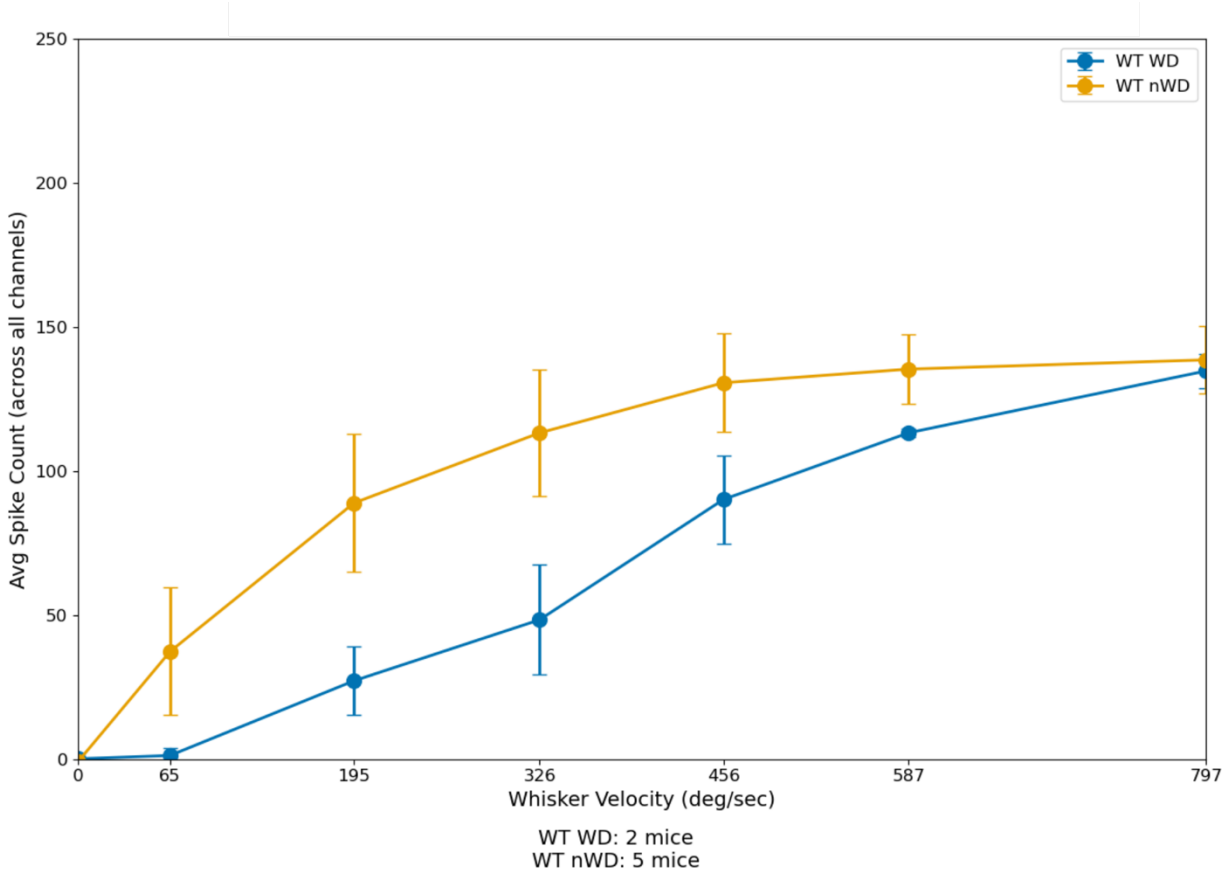


*Figure 7*: Velocity response curve (VRC) for **P21 wildtype subject barrel**s comparing whisker deprivation and non-whisker deprivation. The y-axis represents the average spike counts across all channels for all files at each velocity pertaining to a specific experimental group, and the x-axis represents the varying stimuli velocities utilized from 0 to 800 degrees per section. The error bars shown for each point represent the standard error of the mean (SEM). * Indicates a Mann-Whitney U test significance of $p<0.05$.

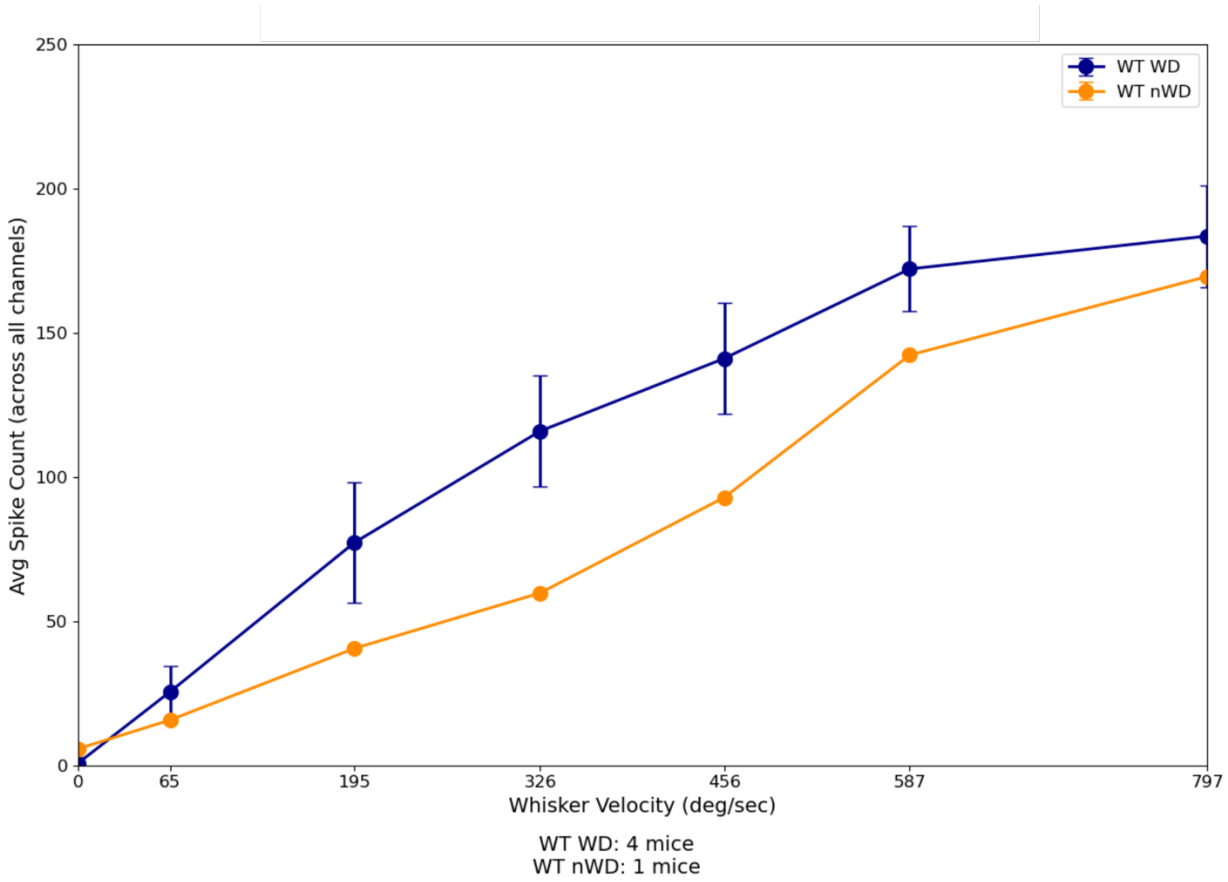


*Figure 8:* Velocity response curve (VRC) for **P21 wildtype subject septa** comparing whisker deprivation and non-whisker deprivation. The y-axis represents the average spike counts across all channels for all files at each velocity pertaining to a specific experimental group, and the x-axis represents the varying stimuli velocities utilized from 0 to 800 degrees per section. The error bars shown for each point represent the standard error of the mean (SEM). * Indicates a Mann-Whitney U test significance of $p<0.05$.

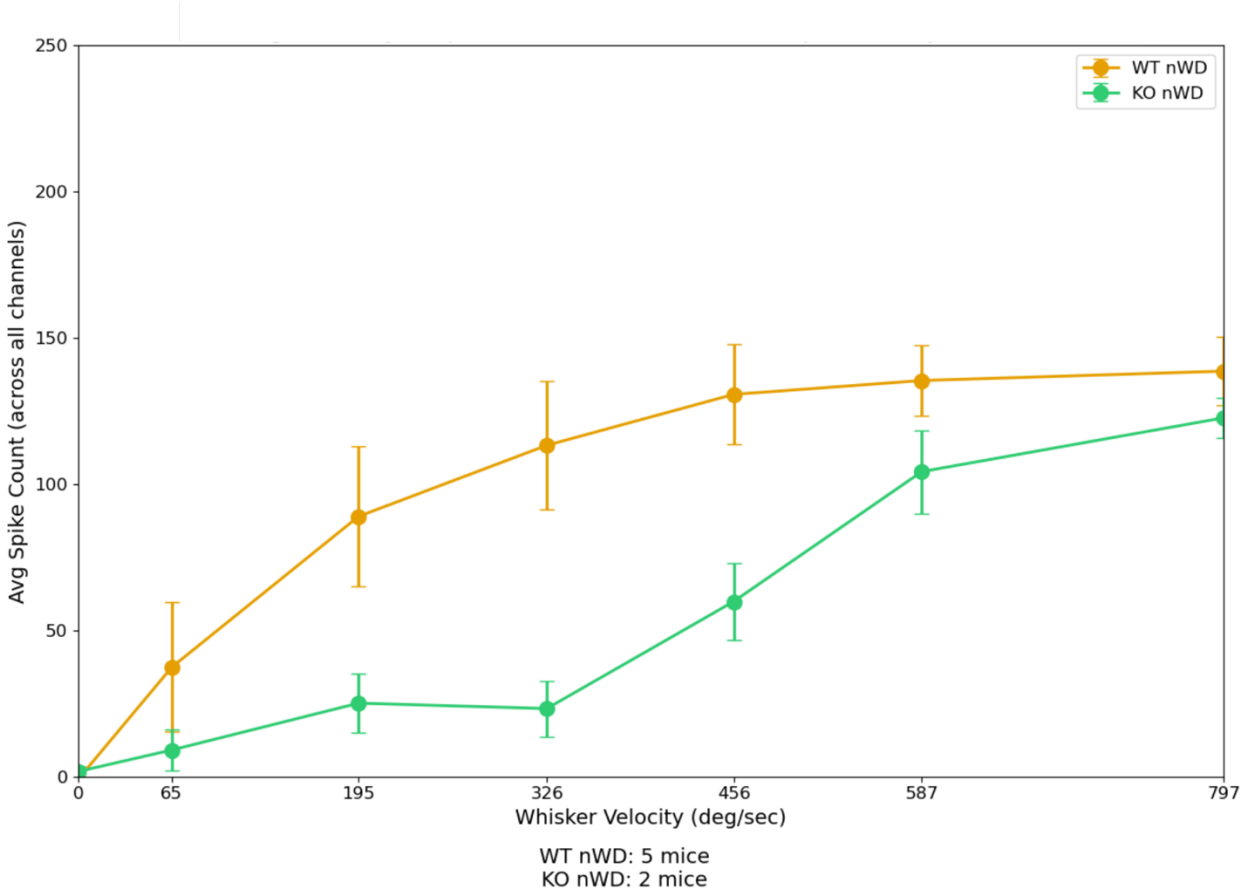


*Figure 9:* Velocity response curve (VRC) for **P21 non-whisker-deprived subject barrels** comparing wildtype and knockout genotypes. The y-axis represents the average spike counts across all channels for all files at each velocity pertaining to a specific experimental group, and the x-axis represents the varying stimuli velocities utilized from 0 to 800 degrees per section. The error bars shown for each point represent the standard error of the mean (SEM). * Indicates a Mann-Whitney U test significance of $p<0.05$.

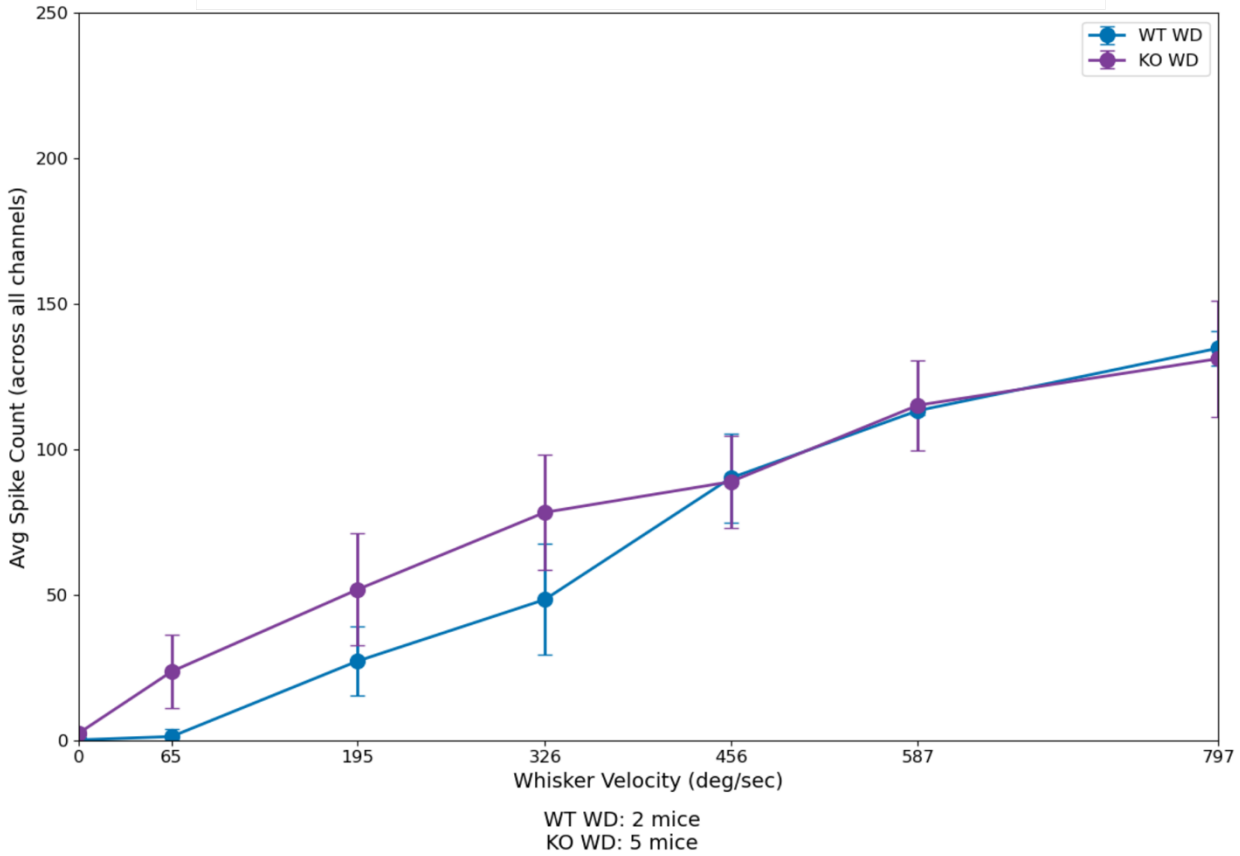


*Figure 10:* Velocity response curve (VRC) for **P21 whisker-deprived subject barrels** comparing wildtype and knockout genotypes. The y-axis represents the average spike counts across all channels for all files at each velocity pertaining to a specific experimental group, and the x-axis represents the varying stimuli velocities utilized from 0 to 800 degrees per section. The error bars shown for each point represent the standard error of the mean (SEM). * Indicates a Mann-Whitney U test significance of $p<0.05$.

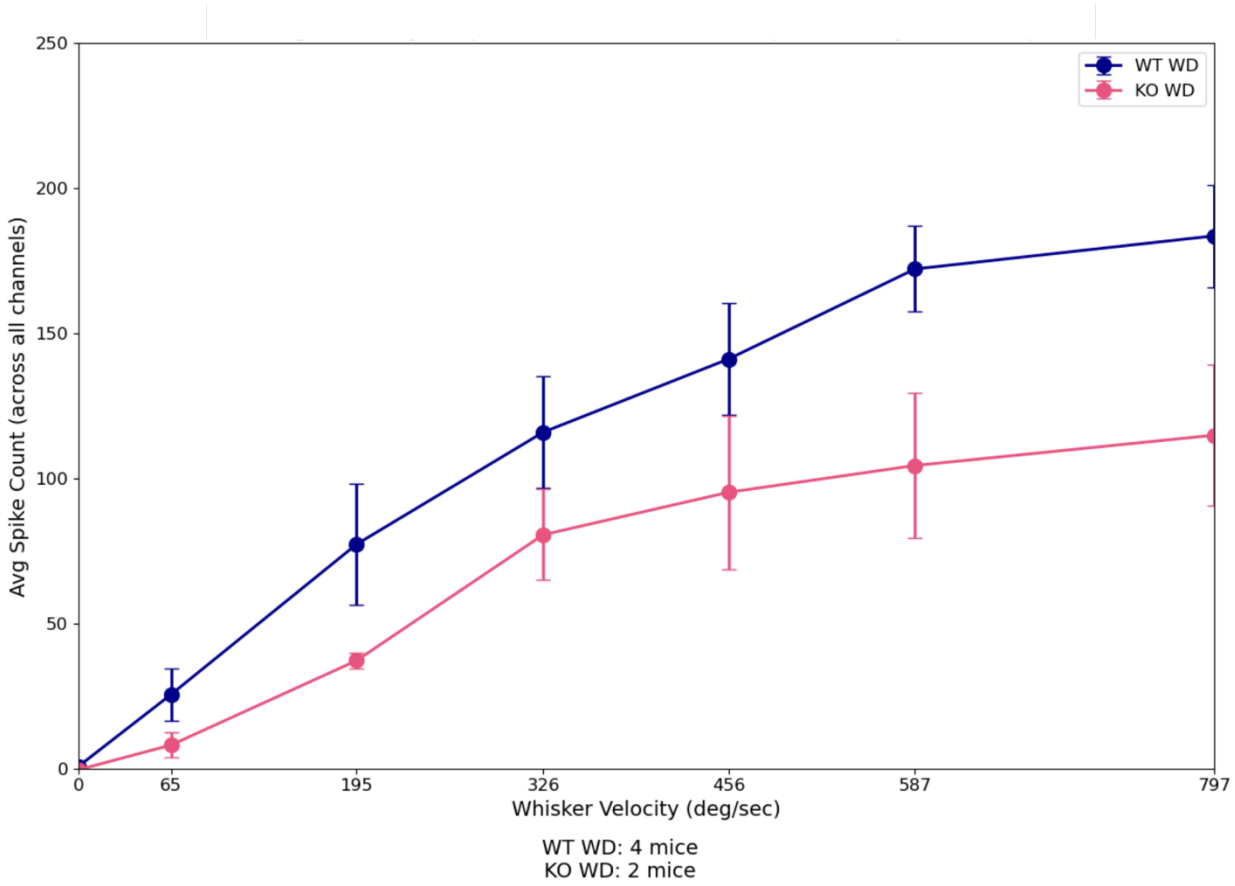


*Figure 11:* Velocity response curve (VRC) for **P21 whisker-deprived subject septa** comparing wildtype and knockout genotypes. The y-axis represents the average spike counts across all channels for all files at each velocity pertaining to a specific experimental group, and the x-axis represents the varying stimuli velocities utilized from 0 to 800 degrees per section. The error bars shown for each point represent the standard error of the mean (SEM). * Indicates a Mann-Whitney U test significance of $p<0.05$.

## Works Cited


Agmon, A., & Connors, B. W. (1991). Thalamocortical responses of mouse somatosensory (barrel) Cortexin Vitro. *Neuroscience*, *41*(2–3), 365–379. https://doi.org/10.1016/0306-4522(91)90333-j

Alloway, K. D. (2007). Information processing streams in rodent barrel cortex: The differential functions of barrel and septal circuits. *Cerebral Cortex*, *18*(5), 979–989. https://doi.org/10.1093/cercor/bhm138

Antoine, M. W., Langberg, T., Schnepel, P., & Feldman, D. E. (2019). Increased excitation-inhibition ratio stabilizes synapse and circuit excitability in four autism mouse models. *Neuron*, *101*(4). https://doi.org/10.1016/j.neuron.2018.12.026

Bear, M. F., Huber, K. M., & Warren, S. T. (2004). The mglur theory of Fragile X mental retardation. *Trends in Neurosciences*, *27*(7), 370–377. https://doi.org/10.1016/j.tins.2004.04.009

Brecht, M., & Sakmann, B. (2002). -dynamic representation of whisker deflection by synaptic potentials in spiny stellate and pyramidal cells in the barrels and septa of layer 4 rat somatosensory cortex. *The Journal of Physiology*, *543*(1), 49–70. https://doi.org/10.1113/jphysiol.2002.018465

Bureau, I., Shepherd, G. M., & Svoboda, K. (2008). Circuit and Plasticity Defects in the Developing Somatosensory Cortex of*Fmr1*Knock-Out Mice. *The Journal of Neuroscience*, *28*(20), 5178–5188. https://doi.org/10.1523/jneurosci.1076-08.2008

Bülow, P., Murphy, T. J., Bassell, G. J., & Wenner, P. (2019). Homeostatic intrinsic plasticity is functionally altered in fmr1 ko cortical neurons. *Cell Reports*, *26*(6). https://doi.org/10.1016/j.celrep.2019.01.035c

Contractor, A., Klyachko, V. A., & Portera-Cailliau, C. (2015). Altered neuronal and circuit excitability in Fragile X syndrome. *Neuron*, *87*(4), 699–715. https://doi.org/10.1016/j.neuron.2015.06.017

Deosthale, P., Balanta-Melo, J., Creecy, A., Liu, C., Marcial, A., Morales, L., Cridlin, J., Robertson, S., Okpara, C., Sanchez, D. J., Ayoubi, M., Lugo, J. N., Hernandez, C. J., Wallace, J. M., & Plotkin, L. I. (2023). Fragile X messenger ribonucleoprotein 1 (FMR1), a novel inhibitor of osteoblast/osteocyte differentiation, regulates bone formation, mass, and strength in young and aged male and female mice. *Bone Research*, *11*(1). https://doi.org/10.1038/s41413-023-00256-x

Desai, N. S. (2003). Homeostatic plasticity in the CNS: Synaptic and intrinsic forms. *Journal of Physiology-Paris*, *97*(4–6), 391–402. https://doi.org/10.1016/j.jphysparis.2004.01.005

Desai, N. S., Rutherford, L. C., & Turrigiano, G. G. (1999). Plasticity in the intrinsic excitability of cortical pyramidal neurons. *Nature Neuroscience*, *2*(6), 515–520. https://doi.org/10.1038/9165

Erzurumlu, R. S., & Gaspar, P. (2012). Development and critical period plasticity of the barrel cortex. *European Journal of Neuroscience*, *35*(10), 1540–1553. https://doi.org/10.1111/j.1460-9568.2012.08075.x

Fox, K., & Stryker, M. (2017). Integrating Hebbian and homeostatic plasticity: Introduction. *Philosophical Transactions of the Royal Society B: Biological Sciences*, *372*(1715), 20160413. https://doi.org/10.1098/rstb.2016.0413

Glazewski, S., Greenhill, S., & Fox, K. (2017). Time-course and mechanisms of homeostatic plasticity in layers 2/3 and 5 of the barrel cortex. *Philosophical Transactions of the Royal*

*Society B: Biological Sciences*, *372*(1715), 20160150. https://doi.org/10.1098/rstb.2016.0150

Jacob, V., Estebanez, L., Le Cam, J., Tiercelin, J.-Y., Parra, P., Parésys, G., & Shulz, D. E. (2010). The matrix: A new tool for probing the whisker-to-barrel system with natural stimuli. *Journal of Neuroscience Methods*, *189*(1), 65–74. https://doi.org/10.1016/j.jneumeth.2010.03.020

Jamann, N., Dannehl, D., Lehmann, N., Wagener, R., Thielemann, C., Schultz, C., Staiger, J., Kole, M. H., & Engelhardt, M. (2021). Sensory input drives rapid homeostatic scaling of the axon initial segment in mouse barrel cortex. *Nature Communications*, *12*(1). https://doi.org/10.1038/s41467-020-20232-x

Kaufmann, W. E., Kidd, S. A., Andrews, H. F., Budimirovic, D. B., Esler, A., Haas-Givler, B., Stackhouse, T., Riley, C., Peacock, G., Sherman, S. L., Brown, W. T., & Berry-Kravis, E. (2017). Autism spectrum disorder in fragile X syndrome: Cooccurring conditions and current treatment. *Pediatrics*, *139*(Supplement_3). https://doi.org/10.1542/peds.2016-1159f

Kim, T., Oh, W. C., Choi, J. H., & Kwon, H.-B. (2016). Emergence of functional subnetworks in layer 2/3 cortex induced by sequential spikes in vivo. *Proceedings of the National Academy of Sciences*, *113*(10). https://doi.org/10.1073/pnas.1513410113

Kim, U., & Ebner, F. F. (1999). Barrels and septa: Separate circuits in rat barrel field cortex. *The Journal of Comparative Neurology*, *408*(4), 489–505. https://doi.org/10.1002/(sici)1096-9861(19990614)408:4<489::aid-cne4>3.3.co;2-5

Lisman, J. (2017). Glutamatergic synapses are structurally and biochemically complex because of multiple plasticity processes: Long-term potentiation, long-term depression, short-term potentiation and scaling. *Philosophical Transactions of the Royal Society B: Biological Sciences*, *372*(1715), 20160260. https://doi.org/10.1098/rstb.2016.0260

Liu, X., Kumar, V., Tsai, N.-P., & Auerbach, B. D. (2022). Hyperexcitability and homeostasis in fragile X syndrome. *Frontiers in Molecular Neuroscience*, *14*. https://doi.org/10.3389/fnmol.2021.805929

Maenner, M. J., Warren, Z., Williams, A. R., Amoakohene, E., Bakian, A. V., Bilder, D. A., Durkin, M. S., Fitzgerald, R. T., Furnier, S. M., Hughes, M. M., Ladd-Acosta, C. M., McArthur, D., Pas, E. T., Salinas, A., Vehorn, A., Williams, S., Esler, A., Grzybowski, A., Hall-Lande, J., … Shaw, K. A. (2023). Prevalence and characteristics of autism spectrum disorder among children aged 8 years — autism and Developmental Disabilities Monitoring Network, 11 sites, United States, 2020. *MMWR. Surveillance Summaries*, *72*(2), 1–14. https://doi.org/10.15585/mmwr.ss7202a1

Martin, B. S., & Huntsman, M. M. (2012). Pathological plasticity in fragile X syndrome. *Neural Plasticity*, *2012*, 1–12. https://doi.org/10.1155/2012/275630

Moberg, S., & Takahashi, N. (2022). Neocortical Layer 5 subclasses: From cellular properties to roles in behavior. *Frontiers in Synaptic Neuroscience*, *14*. https://doi.org/10.3389/fnsyn.2022.1006773

Niere, F., Wilkerson, J. R., & Huber, K. M. (2012). Evidence for a fragile X mental retardation protein-mediated translational switch in metabotropic glutamate receptor-triggered arc translation and long-term depression. *The Journal of Neuroscience*, *32*(17), 5924–5936. https://doi.org/10.1523/jneurosci.4650-11.2012

Petersen, C. C. H. (2007). The functional organization of the barrel cortex. *Neuron*, *56*(2), 339–355. https://doi.org/10.1016/j.neuron.2007.09.017

Petersen, C. C., & Sakmann, B. (2000). The excitatory neuronal network of rat layer 4 barrel cortex. *The Journal of Neuroscience*, *20*(20), 7579–7586. https://doi.org/10.1523/jneurosci.20-20-07579.2000

Rice, F. L., & Van Der Loos, H. (1977). Development of the barrels and barrel field in the somatosensory cortex of the mouse. *The Journal of Comparative Neurology*, *171*(4), 545–560. https://doi.org/10.1002/cne.901710408

Richter, J. D., & Zhao, X. (2021). The molecular biology of FMRP: New Insights Into Fragile X syndrome. *Nature Reviews Neuroscience*, *22*(4), 209–222. https://doi.org/10.1038/s41583-021-00432-0

Rogers, S. J., Wehner, E. A., & Hagerman, R. (2001). The behavioral phenotype in Fragile X: Symptoms of autism in very young children with Fragile X syndrome, idiopathic autism, and other developmental disorders. *Journal of Developmental & Behavioral Pediatrics*, *22*(6), 409–417. https://doi.org/10.1097/00004703-200112000-00008

Scala, F., Kobak, D., Shan, S., Bernaerts, Y., Laturnus, S., Cadwell, C. R., Hartmanis, L., Froudarakis, E., Castro, J. R., Tan, Z. H., Papadopoulos, S., Patel, S. S., Sandberg, R., Berens, P., Jiang, X., & Tolias, A. S. (2019). Layer 4 of mouse neocortex differs in cell types and circuit organization between sensory areas. *Nature Communications*, *10*(1). https://doi.org/10.1038/s41467-019-12058-z

Shai, A. S., Anastassiou, C. A., Larkum, M. E., & Koch, C. (2015). Physiology of layer 5 pyramidal neurons in mouse primary visual cortex: Coincidence detection through bursting. *PLOS Computational Biology*, *11*(3). https://doi.org/10.1371/journal.pcbi.1004090

Sieben, K., Bieler, M., Röder, B., & Hanganu-Opatz, I. L. (2015). Neonatal restriction of tactile inputs leads to long-lasting impairments of cross-modal processing. *PLOS Biology*, *13*(11). https://doi.org/10.1371/journal.pbio.1002304

Soden, M. E., & Chen, L. (2010). Fragile X protein FMRP is required for homeostatic plasticity and regulation of synaptic strength by retinoic acid. *The Journal of Neuroscience*, *30*(50), 16910–16921. https://doi.org/10.1523/jneurosci.3660-10.2010

Staiger, J. F., & Petersen, C. C. (2021). Neuronal circuits in barrel cortex for whisker sensory perception. *Physiological Reviews*, *101*(1), 353–415. https://doi.org/10.1152/physrev.00019.2019

Turnock, A., Langley, K., & Jones, C. R. G. (2022). Understanding stigma in autism: A narrative review and theoretical model. *Autism in Adulthood*, *4*(1), 76–91. https://doi.org/10.1089/aut.2021.0005

Turrigiano, G. G., Leslie, K. R., Desai, N. S., Rutherford, L. C., & Nelson, S. B. (1998). Activity-dependent scaling of quantal amplitude in neocortical neurons. *Nature*, *391*(6670), 892–896. https://doi.org/10.1038/36103

Turrigiano, G. (2011). Homeostatic synaptic plasticity: Local and global mechanisms for stabilizing neuronal function. *Cold Spring Harbor Perspectives in Biology*, *4*(1). https://doi.org/10.1101/cshperspect.a005736

Varani, S., Vecchia, D., Zucca, S., Forli, A., & Fellin, T. (2021). Stimulus feature-specific control of layer 2/3 subthreshold whisker responses by Layer 4 in the mouse primary somatosensory cortex. *Cerebral Cortex*, *32*(7), 1419–1436. https://doi.org/10.1093/cercor/bhab297

Zhang, Z., Marro, S. G., Zhang, Y., Arendt, K. L., Patzke, C., Zhou, B., Fair, T., Yang, N., Südhof, T. C., Wernig, M., & Chen, L. (2018). The fragile X mutation impairs

homeostatic plasticity in human neurons by blocking synaptic retinoic acid signaling. *Science Translational Medicine*, *10*(452). https://doi.org/10.1126/scitranslmed.aar4338